MATHEMATICAL MODELING AND COMPUTING, Vol. 9, No. 3, pp. 616–626 (2022)

The mathematical fractional modeling of TiO_2 nanopowder synthesis by sol–gel method at low temperature

Sadek O., Sadek L., Touhtouh S., Hajjaji A.

Laboratory of Engineering Sciences for Energy, National School of Applied Sciences El Jadida, Chouaib Doukkali University El Jadida, BP 1166, EL Jadida Plateau 24002, Morocco

(Received 6 April 2022; Revised 2 July 2022; Accepted 5 July 2022)

Titanium dioxide is a compound of oxygen and titanium with the formula TiO_2 present in nature and manufactured on an industrial scale. It is used in several fields and applications such as cosmetics, paint, food, photocatalyst, electrodes in lithium batteries, dye solar cells (DSSC), biosensors, etc., given its importance and its various fields of application, there are several methods of synthesis of TiO_2 such as the sol–gel method widely used to obtain nanoparticles. In our study, on the one hand we synthesized titanium dioxide nanopowders crystallized in the anatase phase at a crystal size of 49.25 nm with success using titanium tetraisopropoxide (TTIP) as precursor by the sol–gel method. The powders obtained were analyzed by X-ray diffraction (XRD) with CuK_α radiation ($\lambda = 0.15406$ nm) and Fourier transform infrared spectroscopy (FTIR) in the wave number range $4000 - 400\,cm^{-1}$, and on the other hand we present a mathematical model for the prediction of the TiO_2 concentration as a function of time and the concentration of reactants by using the fractional order derivative more precise than the whole order derivative, we study the existence and the uniqueness of the solutions. In addition, we determine the points of equilibrium. Numerical simulations and their graphical representations are made to visualize the efficiency of this model.

Keywords: *titanium dioxide, sol–gel, nanocrystallized, anatase, XRD, FTIR, fractional model, equilibrium point, fractional calculus, Caputo derivatives.*

2010 MSC: 26A33, 34A08, 34D05, 92D30 **DOI:** 10.23939/mmc2022.03.616

1. Introduction

The wide range of existing and promising applications of nanometric TiO_2, enabled by its many properties, encompasses a whole range of processes involving absorption or diffusion of solar radiation: paint pigments, toothpaste, sun protection; or photo-induced: photocatalysis, detectors, photochromism, electrochromism or photovoltaics. Nanotechnology is the understanding and control of matter at dimensions between approximately 1 and 100 nanometers. Nanocrystalline titanium dioxide or titania is one of the most successful modern functional [1] for a number of technologically important applications, such as catalysis, white pigment for paints or cosmetics, dye-sensitized solar [2], photocatalyst [3], and electrodes in lithium batteries [3]. Titania presents three crystalline phases, rutile (tetragonal structure), anatase (tetragonal structure), and brookite (orthorhombic structure). Figure 1 illustrates the crystallographic structures of different forms of TiO_2 [4].

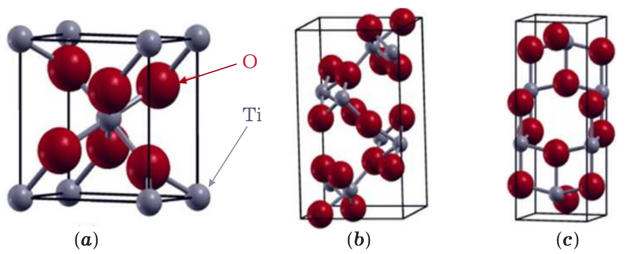

Fig. 1. Crystallographic phases of TiO_2 (***a***) rutile, (***b***) anatase and (***c***) brookite.

In general, TiO_2 is preferred in anatase form because of its high photo catalytic activity, since it has a more negative conduction band edge potential (higher potential energy of photogenerated electrons), high specific area, non-toxic, photochemically stable, and relatively inexpensive [5]. Several methods for the preparation of nanocrystalline TiO_2 have been developed and they are electrochemical reaction [6], supercritical carbon dioxide [7], precipitation [8], multi-gelation [9], chemical solvent and chemical vapor decomposition [10], ultrasonic irradiation [11], aerogel [12], xerogel [13] and sol-gel [14], the latter is the most used because it makes it possible to obtain ultra-fine nanopowder [15–22].

The manuscript is organized as follows: in subsection 2.1, we start with the synthesis of titanium oxide by sol gel method, in subsection 2.2, characterize the powders obtained by X-ray diffraction and Fourier transform infrared spectroscopy, in subsection 2.3, let us recall the reaction diagram of the syntheses of TiO_2 according to the sol-gel method. In subsection 2.4, we present a mathematical model according to these chemical reactions. In subsection 2.5, we present a fractional order model with the Caputo fractional derivative. In subsection 2.6, we study the existence and the uniqueness of solutions. In subsection 2.6, we study the determination of equilibrium points and in the last section we illustrate our model by numerical simulation and compare it to real data.

2. Materials and Methods

2.1. Synthesis of the TiO_2 nanopowders

In this section, we synthesized TiO_2 nanopowders by the sol-gel method using the following reagents: titanium tetraisopropoxide, 2-propanol and distilled water, with a reflux of 70°C. The gel obtained was dried at 70°C for approximately 16 hours to evaporate the solvent, then calcined in an oven to give the TiO_2 nanopowder (rutile, anatase ou brookite), in this work the calcination is at 500°C for to give the anatase nanopowder [13]. These steps are explained in Figure 2.

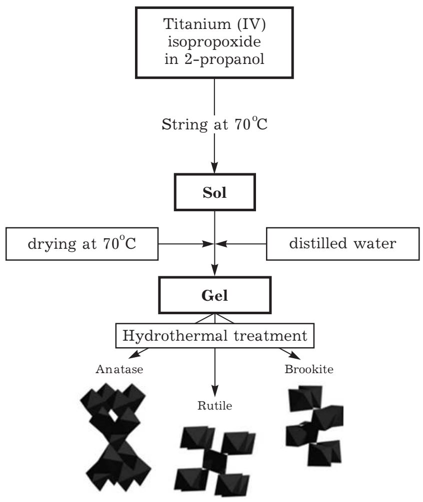

Fig. 2. Schematic flowchart illustrating the synthesis step of titanium dioxide nanomaterials by sol-gel method.

2.2. Characterized of the TiO_2 nanopowders

The TiO_2 synthesized is characterized by X-ray diffraction using CuK_α radiation ($\lambda = 0.15406\,\text{nm}$) and Fourier transform infrared spectroscopy in the wavenumber range $4000 - 400\,\text{cm}^{-1}$.

2.3. Reaction scheme

The sol-gel process involves the evolution of inorganic networks through the formation of a colloidal suspension (Sol) and gelation of the sol to form a network in a continuous liquid phase (Gel). Sol is a dispersion of the solid particles, with a diameter of 11000 nm, in a liquid where only the Brownian motions kept particles in suspension. While a gel is a state where both liquid and solid are dispersed in each other, which presents a solid network filled with liquid components [23]. The wet gel is converted into a dense ceramic with further drying and heat treatment. In this method, the precursors are usually inorganic metal salts or metal–organic compounds such as metal alkoxides. The reaction scheme is usually written as follows:

— Hydrolysis:

$$\underbrace{\text{Ti-OR}}_{\text{Titanium isopropoxyde}} + \underbrace{\text{H}_2\text{O}}_{\text{Water}} \longrightarrow \underbrace{\text{Ti-OH}}_{\text{Titanium hydroxide}} + \underbrace{\text{R-OH}}_{\text{Isopropanol}}, \tag{1}$$

— Condensation:

$$\underbrace{\text{Ti-OH}}_{\text{Titanium hydroxide}} + \underbrace{\text{RO-Ti}}_{\text{Titanium isopropoxyde}} \longrightarrow \underbrace{\text{Ti-O-Ti}}_{\text{Titanium dioxide}} + \underbrace{\text{R-OH}}_{\text{Isopropanol}}, \tag{2}$$

$$\underbrace{\text{Ti-OH}}_{\text{Titanium hydroxide}} + \underbrace{\text{HO-Ti}}_{\text{Titanium dioxide}} \longrightarrow \underbrace{\text{Ti-O-Ti}}_{\text{Titanium dioxide}} + \underbrace{\text{H}_2\text{O}}_{\text{Water}}. \tag{3}$$

2.4. Mathematical model

In this section, we present new mathematical model from chemical reactions (1), (2) and (3), are first rewritten as

$$\underbrace{\text{Ti-OR}}_{A} + \underbrace{\text{H}_2\text{O}}_{B} \xrightarrow{k_1} \underbrace{\text{Ti-OH}}_{C} + \underbrace{\text{R-OH}}_{D} \tag{4}$$

$$\underbrace{\text{Ti-OH}}_{C} + \underbrace{\text{RO-Ti}}_{A} \xrightarrow{k_2} \underbrace{\text{Ti-O-Ti}}_{E} + \underbrace{\text{R-OH}}_{D} \tag{5}$$

$$\underbrace{\text{Ti-OH}}_{C} + \underbrace{\text{HO-Ti}}_{C} \xrightarrow{k_3} \underbrace{\text{Ti-O-Ti}}_{E} + \underbrace{\text{H}_2\text{O}}_{B}, \tag{6}$$

where $k_i = \mathbb{A}_i e^{-\mathbb{E}_i/RT}$ [24] is the reaction rate, with $\mathbb{A}_i$ being a pre-exponential factor (not a frequency factor) and $\mathbb{E}_i$ the apparent activation energy, with T is the isokinetic temperature. From chemical reactions (4), (5) and (6) the evolution is modeled by the following system of ordinary differential equations.

$$\begin{cases} \dfrac{dA(t)}{dt} = -k_1 A(t)B(t) - k_2 A(t)C(t), \\ \dfrac{dB(t)}{dt} = -k_1 A(t)B(t) + k_3 C(t)^2, \\ \dfrac{dC(t)}{dt} = k_1 A(t)B(t) - k_2 A(t)C(t) - k_3 C(t)^2, \\ \dfrac{dD(t)}{dt} = k_1 A(t)B(t) + k_2 A(t)C(t), \\ \dfrac{dE(t)}{dt} = k_2 A(t)C(t) + k_3 C(t)^2, \end{cases} \tag{7}$$

with initial conditions:

$$A(0) = A_0, \quad B(0) = B_0, \quad C(0) = C_0, \quad D(0) = D_0 \quad \text{and} \quad E(0) = E_0.$$

2.5. Fractional order model

Many authors have introduced fractional calculus in many works, fractional operators can more accurately express the natural phenomena than their traditional counterpart in [25–32].

Recently, fractional derivatives and integrals have been utilized frequently to critically analyze the main characteristics of the problems in the real world. Many authors have introduced that the fractional operators can more accurately express the natural phenomena than the traditional counterpart. One of the best ways to describe fractional calculus is to present the definition of Caputo fractional derivative in [33]:

$$f^{(\mu)}(t) = \begin{cases} \dfrac{1}{\Gamma(n-\mu)} \displaystyle\int_0^t \frac{f^{(n)}(\tau)}{(t-\tau)^{\mu-n+1}} d\tau, & n-1 < \mu < n \in \mathbb{N}, \\ f^{(n)}(\tau), & \mu = n \in \mathbb{N}, \end{cases} \tag{8}$$

where the Euler's gamma function Γ by the following integral

$$\Gamma(x) = \int_0^\infty e^{-t} t^{x-1}\, dt.$$

The fractional integral having of order $\alpha > 0$ is

$$I^\mu(f(t)) = \frac{1}{\Gamma(\mu)} \int_0^t \frac{f(s)}{(t-s)^{1-\mu}}\, ds,$$

where $t > 0$, satisfies:

$$\begin{cases} (I^\mu f(t))^{(\mu)} = f(t), \\ I^\mu(f(t)^{(\mu)}) = f(t) - f(0). \end{cases} \tag{9}$$

Now, let us present the fractional version of the model by means of the Caputo operator as follows:

$$\begin{cases} A^{(\mu)}(t) = -k_1 A(t)B(t) - k_2 A(t)C(t), \\ B^{(\mu)}(t) = -k_1 A(t)B(t) + k_3 C(t)^2, \\ C^{(\mu)}(t) = k_1 A(t)B(t) - k_2 A(t)C(t) - k_3 C(t)^2, \\ D^{(\mu)}(t) = k_1 A(t)B(t) + k_2 A(t)C(t), \\ E^{(\mu)}(t) = k_2 A(t)C(t) + k_3 C(t)^2. \end{cases} \tag{10}$$

2.6. Existence and uniqueness of solutions

In this section, we prove the existence of the system of solutions. We have

$$\begin{cases} A^{(\mu)}(t) = -D^{(\mu)}(t), \\ A^{(\mu)}(t) + E^{(\mu)}(t) - B^{(\mu)}(t) = 0, \end{cases}$$

so

$$\begin{cases} D(t) = A_0 - A(t), \\ E(t) = B(t) - A(t) + A_0 - B_0. \end{cases}$$

Then, we consider the following subsystem:

$$\begin{cases} A^{(\mu)}(t) = -k_1 A(t)B(t) - k_2 A(t)C(t), \\ B^{(\mu)}(t) = -k_1 A(t)B(t) + k_3 C(t)^2, \\ C^{(\mu)}(t) = k_1 A(t)B(t) - k_2 A(t)C(t) - k_3 C(t)^2. \end{cases} \tag{11}$$

Note $\mathbb{R}^3_+ = \{X \in \mathbb{R}^3 \colon X \geqslant 0\}$ and let $X(t) = (A(t), B(t), C(t))^T$. Then the system (11) can be reformulated as follows:

$$X^{(\alpha)}(t) = F(X(t)), \tag{12}$$

where

$$F(X) = \begin{pmatrix} -k_1 AB - k_2 AC \\ -k_1 AB + k_3 C^2 \\ k_1 AB - k_2 AC - k_3 C^2 \end{pmatrix}. \tag{13}$$

The following lemma found in [34], gives the global existence of the solution of the system (12).

Lemma 1 (Ref. [34]). *Suppose that F satisfies the following conditions:*

a) *$F(X)$ and $\frac{dF}{dX}$ are continuous in $X \in \mathbb{R}^3$;*

b) *$\|F(X)\| \leqslant \omega + \lambda \|X\|, \forall X \in \mathbb{R}^3$, where ω and λ are two positive constants.*

The system (12) admits a unique solution on $[0, +\infty[$.

Theorem 1. *There exists a unique solution for equation (11).*

Proof. Since the vector function F in (13) satisfies the first condition of Lemma 1, it suffices to dismantle the second. And $\|F(X)\| \leqslant v\|X\|$, where v is constant. ■

2.7. Equilibrium points

To determine the equilibrium points of the fractional-order system (11), we solve the following equations:

$$A^{(\mu)}(t) = B^{(\mu)}(t) = C^{(\mu)}(t) = 0. \tag{14}$$

By solving the algebraic equation (14), we obtain equilibrium points of the system (10). So,

$$\begin{aligned} A(k_1 B + k_2 C) &= 0, \\ -k_1 AB + k_3 C^2 &= 0, \\ k_1 AB - k_2 AC - k_3 C^2 &= 0, \end{aligned}$$

we obtain

— if $A = 0$, so $C = 0$;
— if $A \neq 0$, so $k_1 B + k_2 C = 0$ then $B = C = 0$.

Then the equilibrium points:

$$\begin{aligned} \mathcal{E}_1 &= (0, B^*, 0, D^*, E^*), \\ \mathcal{E}_2 &= (A^*, 0, 0, D^*, E^*). \end{aligned}$$

3. Results and discussion

3.1. Characterized of TiO_2 nanopowders

Figure 3 shows the FTIR spectrum of the TiO_2 nanopowders. It indicates the presence of a band due to the stretching vibrations of the Ti-O-Ti and Ti-O bonds between 500 and 600 cm^{-1} [35], which indicates the formation of TiO_2 nanopowders.

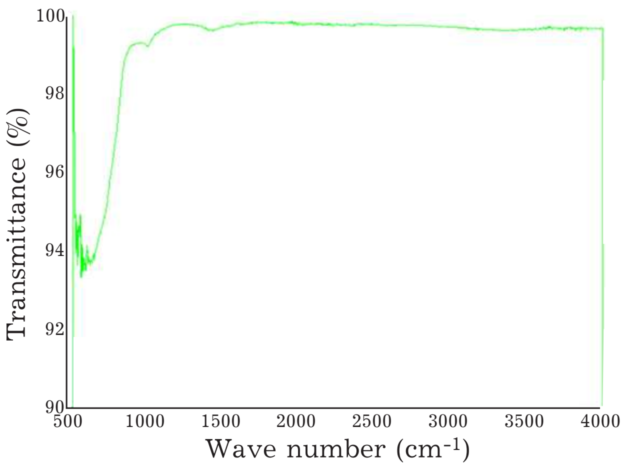

Fig. 3. FTIR of titanium dioxide nanomaterials.

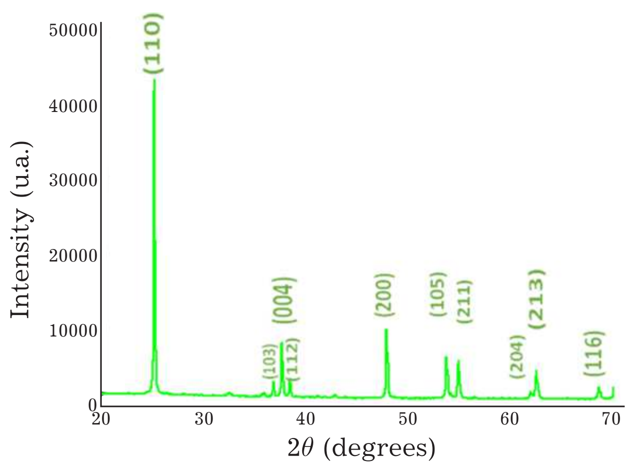

Fig. 4. XRD of titanium dioxide nanomaterials.

Figure 4 of the XRD diffractogram shows the presence of an intense peak of 2θ about 25° corresponding to the plane (101) of the anatase phase, which shows that this TiO_2 nanopowders is formed in an anatase phase. the other peaks correspond respectively to the planes: (103), (004), (112), (200), (105), (211), (213), (204) and (116) of the anatase phase [36]. The average crystallite size ν calculated using the Scherrer equation: $\nu = \frac{K\lambda}{\beta\cos(\theta)}$ is 48.9 nm [37]. These results show that TiO_2 nanopowders in an anatase phase were obtained with suckers by the sol-gel method.

3.2. Numerical simulations

Numerical simulations for fractional order model using predictor-corrector method for fractional differential equations in [38] on a laptop with an Intel Core i3 processor and 4GB of RAM. Since molar concentration of A, B, C, D and E are considered nonnegative, where A_0 and B_0 must be nonzero for an chemical reaction. Initial condition $C_0 = D_0 = E_0 = 0$, $A_0 = 12.35\,\text{mol/l}$ and $B_0 = 19.25\,\text{mol/l}$ taken from article in [13], we did the same experiences mentioned in article [13] and the obtained results are shown in Figure 5. For the numerical simulations we take $k_1 = 0.05$, $k_2 = 3$, and $k_3 = 6$.

Figure 5 and Figure 6 present the graphical results of the proposed fractional order model (10) to analyze the influence of the fractional order, as a result we found that the numerical simulations for $\mu = 0.85$ correspond to the values of the experimental data. We also found that $6.74332\,\text{mol/l}$ of TiO_2 was obtained for about 6 hours from $12.35\,\text{mol/l}$ of TiOR and $19.25\,\text{mol/l}$ of H_2O. From Figure 7, we note that the duration of the reaction and the concentration of TiO_2 synthesized depend on the concentration of water used in the reaction, the more the concentration of water increases, the more the concentration of TiO_2 also increases and the reaction will be fast and will take the minimum of time.

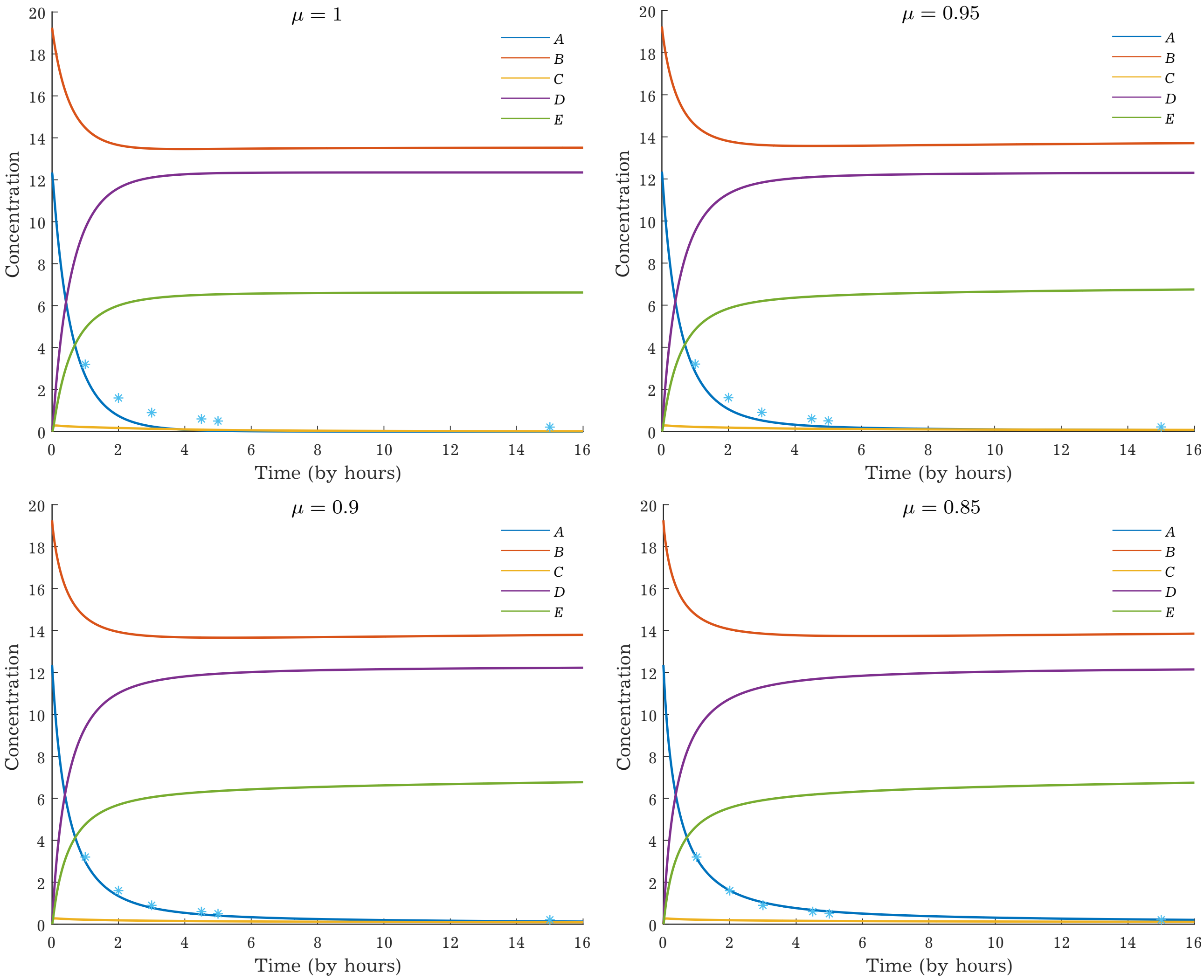

Fig. 5. Temporal variation of reactants and products.

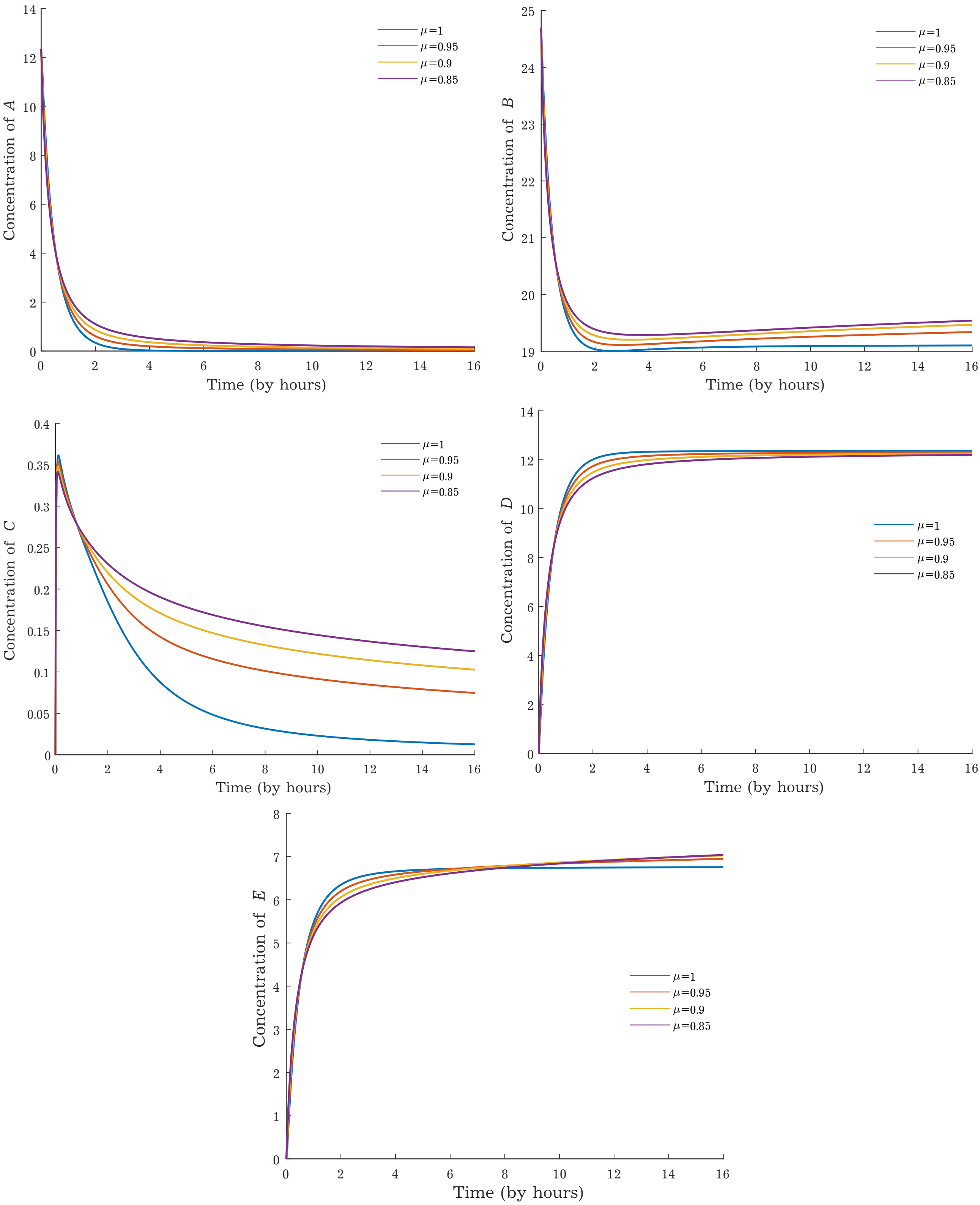

Fig. 6. Analyze the influence of fractional order.

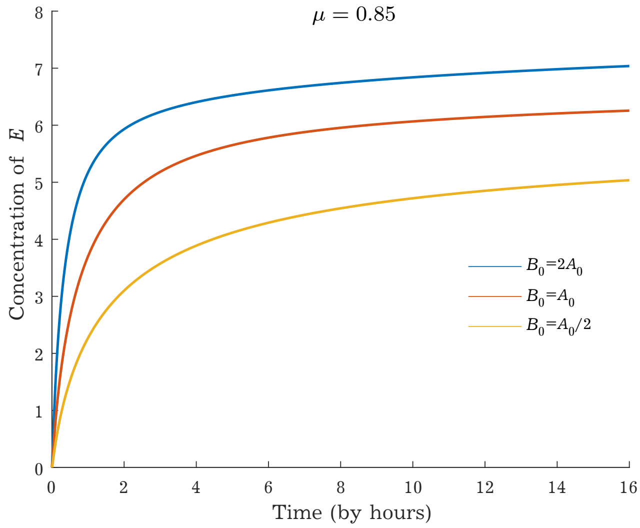

Fig. 7. Temporal variation of titanium dioxide as a function of reagent concentration at $A_0 = 12.35$.

4. Conclusion

In this manuscript, titanium dioxide nanopowders were successfully synthesized by the sol-gel method using titanium tetraisopropoxide as precursor. Analysis of the powders obtained by FTIR and XRD shows that our product is in the form of anatase at crystal sizes of 48.9 nm. For a second part, we presented a mathematical model to analyze the concentration of TiO_2 as a function of time using the fractional derivative; this will help chemists to do without prior experience and knowledge about the interaction. Some interesting results are obtained, on the one hand we found that the values of the experimental data correspond to the fractional order model with $\mu = 0.85$, while on the other hand we found that the duration of the reaction and the concentration of TiO_2 depends on the concentration of H_2O, the more the concentration of H_2O increases, the more the TiO_2 concentration increases and the reaction will be fast and will take the minimum time. In our future work, we intend to study the effect of temperature on this model, and we will apply the obtained nanopowders in an important application.

Acknowledgments

The authors should express their deep-felt thanks to the anonymous referees for their encouraging and constructive comments, which improved this paper.

[1] Ivanova T., Harizanova A., Koutzarova T., Vertruyen B. Optical and structural characterization of TiO_2 films doped with silver nanoparticles obtained by sol–gel method. Optical Materials. **36** (2), 207–213 (2013).

[2] Park H., Kim W.-R., Jeong H.-T., Lee J.-J., Kim H.-G., Choi W.-Y. Fabrication of dye-sensitized solar cells by transplanting highly ordered TiO_2 nanotube arrays. Solar Energy Materials and Solar Cells. **95** (1), 184–189 (2011).

[3] Ochiai T., Fujishima A. Photoelectrochemical properties of TiO_2 photocatalyst and its applications for environmental purification. Journal of Photochemistry and Photobiology C: Photochemistry Reviews. **13** (4), 247–262 (2012).

[4] Armstrong A. R., Armstrong G., Canales J., Bruce P. G. TiO_2–B nanowires as negative electrodes for rechargeable lithium batteries. Journal of Power Sources. **146** (1–2), 501–506 (2005).

[5] Macwan D. P., Dave P. N., Chaturvedi S. A review on nano-TiO_2 sol–gel type syntheses and its applications. Journal of materials science. **46** (11), 3669–3686 (2011).

[6] Wang S., Wu X., Qin W., Jiang Z. TiO_2 films prepared by micro-plasma oxidation method for dye-sensitized solar cell. Electrochimica Acta. **53** (4), 1883–1889 (2007).

[7] Wu C.-I., Huang J.-W., Wen Y.-L., Wen S. B., Shen Y.-H., Yeh M.-Y. Preparation of TiO_2 nanoparticles by supercritical carbon dioxide. Materials Letters. **62** (12–13), 1923–1926 (2008).

[8] Kim S. J., Park S. D., Jeong Y. H., Park S. Homogeneous precipitation of TiO_2 ultrafine powders from aqueous $TiOCl_2$ solution. Journal of the American Ceramic Society. **82** (4), 927–932 (1999).

[9] Neppolian B., Yamashita H., Okada Y., Nishijima H., Anpo M. Preparation of unique TiO_2 nano-particle photocatalysts by a multi-gelation method for control of the physicochemical parameters and reactivity. Catalysis Letters. **105** (1), 111–117 (2005).

[10] Ghorai T. K., Dhak D., Biswas S. K., Dalai S., Pramanik P. Photocatalytic oxidation of organic dyes by nano-sized metal molybdate incorporated titanium dioxide ($M_xMo_xTi_{1-x}O_6$) (M = Ni, Cu, Zn) photocatalysts. Journal of Molecular Catalysis A: Chemical. **273** (1–2), 224–229 (2007).

[11] Peng F., Cai L., Yu H., Wang H., Yang J. Synthesis and characterization of substitutional and interstitial nitrogen-doped titanium dioxides with visible light photocatalytic activity. Journal of Solid State Chemistry. **181** (1), 130–136 (2008).

[12] Bruns W., Ichim B., Söger C. The power of pyramid decomposition in Normaliz. Journal of Symbolic Computation. **74**, 513–536 (2016).

[13] Nachit W., Touhtouh S., Ramzi Z., Zbair M., Eddiai A., Rguiti M., Bouchikhi A., Hajjaji A., Benkhouja K. Synthesis of nanosized TiO_2 powder by sol gel method at low temperature. Molecular Crystals and Liquid Crystals. **627** (1), 170–175 (2016).

[14] Crişan M., Brăileanu A., Răileanu M., Zaharescu M., Crişan D., Drăgan N., Anastasescu M., Ianculescu A., Niţoi I., Marinescu V. E., Hodorogea S. M. Sol–gel S-doped TiO_2 materials for environmental protection. Journal of Non-Crystalline Solids. **354** (2–9), 705–711 (2008).

[15] Sadek O., Touhtouh S., Hajjaji A. The Rapid Identification of Solid Materials Using the ACP Method. Environmental Sciences Proceedings. **16** (1), 22 (2022).

[16] Sadek O., Touhtouh S., Mahdi Bouabdalli E., Hajjaji A. Development of a protocol for the rapid identification of solid materials using the principal component analysis (ACP) method: Case of phosphate fertilizers. Materials Today: Proceedings (2022).

[17] Bouabdalli E. M., El Jouad M., Touhtouh S., Sadek O., Hajjaji A. Structural studies on varied concentrations of europium doped strontium phosphate glasses. Materials Today: Proceedings (2022).

[18] Horikawa T., Katoh M., Tomida T. Preparation and characterization of nitrogen-doped mesoporous titania with high specific surface area. Microporous and Mesoporous Materials. **110** (2–3), 397–404 (2008).

[19] Kim B.-H., Lee J.-Y., Choa Y.-H., Higuchi M., Mizutani N. Preparation of TiO_2 thin film by liquid sprayed mist CVD method. Materials Science and Engineering: B. **107** (3), 289–294 (2004).

[20] Muscat J., Swamy V., Harrison N. M. First-principles calculations of the phase stability of TiO_2. Physical Review B. **65** (22), 224112 (2002).

[21] Mo S.-D., Ching W. Y. Electronic and optical properties of three phases of titanium dioxide: Rutile, anatase, and brookite. Physical Review B. **51** (19), 13023 (1995).

[22] Ohno T., Akiyoshi M., Umebayashi T., Asai K., Mitsui T., Matsumura M. Preparation of S-doped TiO_2 photocatalysts and their photocatalytic activities under visible light. Applied Catalysis A: General. **265** (1), 115–121 (2004).

[23] Prasad K., Pinjari D. V., Pandit A. B., Mhaske S. T. Phase transformation of nanostructured titanium dioxide from anatase-to-rutile via combined ultrasound assisted sol–gel technique. Ultrasonics Sonochemistry. **17** (2), 409–415 (2010).

[24] Graaf G. H., Stamhuis E. J., Beenackers A. A. C. M. Kinetics of low-pressure methanol synthesis. Chemical Engineering Science. **43** (12), 3185–3195 (1988).

[25] Khajji B., Boujallal L., Elhia M., Balatif O., Rachik M. A fractional-order model for drinking alcohol behaviour leading to road accidents and violence. Mathematical Modeling and Computing. **9** (3), 501–518 (2022).

[26] Gouasnouane O., Moussaid N., Boujena S., Kabli K. A nonlinear fractional partial differential equation for image inpainting. Mathematical Modeling and Computing. **9** (3), 536–546 (2022).

[27] Ben-Loghfyry A., Hakim A. Time-fractional diffusion equation for signal and image smoothing. Mathematical Modeling and Computing. **9** (2), 351–364 (2022).

[28] Pawar D. D., Patil W. D., Raut D. K. Fractional-order mathematical model for analysing impact of quarantine on transmission of COVID-19 in India. Mathematical Modeling and Computing. **8** (2), 253–266 (2021).

[29] Fadugba S. E., Ali F., Abubakar A. B. Caputo fractional reduced differential transform method for SEIR epidemic model with fractional order. Mathematical Modeling and Computing. **8** (3), 537–548 (2021).

[30] Kostrobij P. P., Markovych B. M., Ryzha I. A., Tokarchuk M. V. Generalized kinetic equation with spatio-temporal nonlocality. Mathematical Modeling and Computing. **6** (2), 289–296 (2019).

[31] Kostrobij P., Markovych B., Viznovych O., Zelinska I., Tokarchuk M. Generalized Cattaneo–Maxwell diffusion equation with fractional derivatives. Dispersion relations. Mathematical Modeling and Computing. **6** (1), 58–68 (2019).

[32] Odibat Z. M., Shawagfeh N. T. Generalized Taylor's formula. Applied Mathematics and Computation. **186** (1), 286–293 (2007).

[33] Samko S. G., Kilbas A. A., Marichev O. I. Fractional integrals and derivatives. Vol. 1. Yverdon-les-Bains, Switzerland: Gordon and breach science publishers, Yverdon (1993).

[34] Lin W. Global existence theory and chaos control of fractional differential equations. Journal of Mathematical Analysis and Applications. **332** (1), 709–726 (2007).

[35] Kim W. B., Choi S. H., Lee J. S. Quantitative Analysis of Ti-O-Si and Ti-O-Ti Bonds in Ti-Si Binary Oxides by the Linear Combination of XANES. Journal of Physical Chemistry B. **104** (36), 8670–8678 (2000).

[36] Suppuraj P., Parthiban S., Swaminathan M., Muthuvel I. Hydrothermal fabrication of ternary NrGO-$TiO_2/ZnFe_2O_4$ nanocomposites for effective photocatalytic and fuel cell applications. Materials Today: Proceedings. **15** (3), 429–437 (2019).

[37] Himabindu B., Devi N. L., Kanth B. R. Microstructural parameters from X-ray peak profile analysis by Williamson–Hall models; A review. Materials Today: Proceedings. **47** (14), 4891–4896 (2021).

[38] Garrappa R. On linear stability of predictor–corrector algorithms for fractional differential equations. International Journal of Computer Mathematics. **87** (10), 2281–2290 (2010).

Математичне дробове моделювання синтезу нанопорошку TiO_2 золь–гель методом за низьких температур

Садек О., Садек Л., Тотух С., Хаджаджі А.

Лабораторія інженерних наук для енергетики, Національна школа прикладних наук Ель-Джадіда, Університет Шуайб Дуккалі Ель-Джадіда, BP 1166, плато Ель-Джадіда 24002, Марокко

Діоксид титану — це сполука кисню і титану з формулою TiO_2, яка є в природі та виготовляється у промислових масштабах. Він використовується в декількох галузях і сферах застосування, таких як косметика, фарби, продукти харчування, фотокаталізатор, електроди в літієвих батареях, сонячні батареї на барвнику (DSSC), біосенсори тощо. Враховуючи його важливість і різні сфери застосування, існує декілька методів синтез TiO_2, наприклад, золь–гель метод, який широко використовується для отримання наночастинок. У нашому дослідженні, з одного боку, успішно синтезовано нанопорошки діоксиду титану, кристалізовані у фазі анатазу з розміром кристалів 49.25 нм, використовуючи тетраізопропоксид титану (TTIP) як попередник золь–гель метода. Отримані порошки аналізували методом рентгенівської дифракції (XRD) з CuK_α випромінюванням ($\lambda = 0.15406$ нм) та інфрачервоною спектроскопією з перетворенням Фур'є (FTIR) в діапазоні хвильових чисел $4000-400\,\mathrm{cm}^{-1}$, а з іншого боку, представлено математичну модель для передбачення концентрації TiO_2 як функції часу та концентрації реагентів за допомогою дробової похідної, більш точної, ніж похідна цілого порядку; досліджено існування та єдиність розв'язків. Крім того, визначено точки рівноваги. Для візуалізації ефективності цієї моделі виконано числове моделювання та їх графічне представлення.

Keywords: *діоксид титану, золь–гель, нанокристалізований, анатаз, дифракція X-променів, ІЧ-Фур'є, дробова модель, точка рівноваги, дробове числення, похідні Капуто.*